

Closer in the Gap: Towards Portable Performance on RISC-V Vector Processors

Ruimin Shi¹[0009-0003-4387-367X], Maya Gokhale²[0000-0003-4229-5735],
Pei-Hung Lin²[0000-0003-4977-814X], Xavier Teruel³[0000-0001-5181-7545], and
Ivy Peng¹[0000-0003-4158-3583] ✉

¹ KTH Royal Institute of Technology, Sweden {ruimins, ivybopeng}@kth.se

² Lawrence Livermore National Laboratory, USA {gokhale2, lin32}@llnl.gov

³ Barcelona Supercomputing Center, Spain xavier.teruel@bsc.es

Abstract. The RISC-V Vector Extension (RVV) is a cornerstone for sustaining compute throughout in scientific and machine learning workloads. However, compiler support and performance monitoring on RVV 1.0 hardware remain actively evolving. In this work, we design a suite of assembly microbenchmarks to calibrate performance counters on the BananaPi-F3 RVV hardware. Using the benchmarks, we find that predication overhead and stride load pose performance bottlenecks that current compiler cost models do not yet fully capture. Evaluating GCC 15 and Clang 21 across six scientific and ML applications, GCC 15 produces more stable and efficient code generation, outperforming Clang 21 in four of six benchmarks. Clang 21 achieves superior performance only in SGEMM and DGEMM, attributable to more aggressive instruction reduction as confirmed by our validated perf counters. Default LMUL selection proves near-optimal in most cases, though GCC 15 shows greater potential for performance gains through larger LMUL tuning than Clang 21. Finally, we contribute an RVV backend for Google’s Qsim quantum circuit simulator implemented using RVV intrinsics, where GCC 15 again outperforms LLVM 21 on this complex, real-world workload.

1 Introduction

The RISC-V Instruction Set Architecture (ISA) has attracted increasing interest from both industry and academia for its open, modular design and suitability for workload-specific customization [15, 5, 10, 13]. A cornerstone of RISC-V’s relevance to High-Performance Computing is the *RISC-V Vector Extension* (RVV). Many HPC workloads, including ML training and inference, scientific simulations, and signal processing, are built around data-parallel algorithms that benefit directly from wide vector execution. Unlike traditional SIMD with fixed vector lengths in ISA, RVV adopts a *Vector-Length-Agnostic* (VLA) model where the active vector length can be determined at runtime. Another popular VLA realization is ARM’s scalable vector extension (SVE), which was first implemented in Fujitsu’s A64FX processor powering the Fugaku supercomputer, and widely adopted in recent NVIDIA Grace and AWS Graviton processors [16].

For achieving portable performance on various RVV hardware, compiler support and performance profiling are both important. Auto-vectorization compiler support is the key enabler for portable performance on broad RVV hardware. At the fast pace of new RVV hardware emerging, compiler support allows applications to harness different vector hardware without rewriting applications. However, compared to vector length-specific SIMD, RVV’s VLA model imposes new challenges on the compiler support for auto-vectorization. One particular challenge is that under uncertainty about the hardware vector width at compilation time, a compiler must generate correct `vsetvl` sequences that set active vector length at runtime, select an appropriate value for the vector length multiplier (LMUL), and handle tail elements and masks. Addressing these difficulties, GNU and LLVM are both under active development to ramp up RVV support.

Prior works have characterized compiler support for RVV, including comparative evaluations of GCC 14 and LLVM 19 on ratified RVV 1.0 hardware [1, 10, 6]. However, both compilers have since undergone substantial RVV-specific development. For instance, GCC 15 introduced early-break loop vectorization, corrected memory misaligned access, and dynamic LMUL selection. LLVM 21 added multiple hardware-specific scheduling models for recent RVV hardware. An up-to-date evaluation of these compiler advances is therefore timely and necessary. Meanwhile, performance monitoring on RISC-V hardware remains significantly less mature than on x86 or AArch64 [3]. The RISC-V specification mandates only two HPM counters, `cycle` and `instruction`, leaving other events to custom-specific implementation. Therefore, validating the availability and reliability of performance monitoring counters remains necessary for optimizing performance on RVV hardware. In this paper, we make the following contributions:

- We design a suite of assembly microbenchmarks targeting key RVV 1.0 arithmetic and data access operations, and validate RVV-specific hardware performance events in *perf* on RVV hardware.
- We evaluate the enhanced support for RVV autovectorization in GCC15 and LLVM21 in six HPC and ML proxy applications on two RVV1.0 hardware.
- We quantify that predication masks introduce 35% overhead w.r.t unmasked `vsetvl` for tailing elements, and strided vector ld/st instructions incur up to 4× the cost of unit-stride equivalents
- We contribute an RVV backend for a production quantum circuit simulator Qsim using RVV intrinsics and find that GCC 15 outperforms LLVM 21 on this complex, real-world workload.

2 Background

RVV Processors and VLA. The RVV version v1.0 [2] was ratified in 2021 and since then, hardware implementation has gained traction in vendors and undergone active development [13]. RVV supports the VLA programming model, similar to ARM scalable vector extension (SVE). Different from vector length specific (VLS), such as x86 AVX and ARM NEON, which require the vector

length known at compilation time, VLA allows the same binary to be portable across RVV hardware with different vector length (VLEN). RVV defines 32 VLEN-bit long vector registers. Recent implementations support VLEN from 128 up to 16384 [13]. Through dynamic register typing, RVV tag data element types and size to vector registers instead of instructions, to enable a fixed ISA supporting growing VLEN. The active vector length (VL) is determined at runtime via the `vsetvl` instruction and depends on the memory allocated to vector registers in hardware implementation, the number of activated vector registers, and the selected element width (SEW). LMUL is a multiplier of values 1/8, 1/4, 1/2, 1, 2, 4, or 8, which groups multiple vector registers into one ‘logical’ vector so that when LMUL is larger than 1, more elements can be executed in one instruction. Combining these architectural parameters, the theoretical maximum number of elements that can be operated on with a single vector instruction is $VL = \frac{LMUL * VLEN}{SEW}$. RVV also provides the masking mechanism to support predicated vector execution and non-unit stride and indexed gather/scatter operations for irregular loop patterns.

Compiler Support for VLA model. RVV intrinsics and autovectorization are the primary mechanisms to translate RVV’s architectural portability into practical performance portability in applications. Both GCC and LLVM have offered code generation compliant with RVV 1.0 specification. A capable compiler can generate code that automatically adapts to the underlying vector hardware at runtime, removing the need for platform-specific hand tuning required by VLS. Both GCC and LLVM have invested heavily in RVV 1.0 support.

The RVV 1.0 C intrinsics provide developers with direct access to individual vector instructions from the C/C++ source code, including control over SEW, LMUL, VL and masks. Intrinsics thus represent the performance ceiling against which compiler-generated autovectorized outcomes can be measured. For irregular access patterns, hand-written intrinsic code consistently outperforms compiler-generated code in earlier LLVM Clang releases. [1].

Compiler autovectorization transforms scalar loops into vector code automatically, selecting appropriate LMUL values, emitting `vsetvl` instructions [6]. GCC 14 and Clang 19 were the first GNU and LLVM releases with production-quality RVV autovectorization and full C intrinsics. GCC 15 extends this with saturating arithmetic (`vssubu.vv`, `vnclipu.wi`), early-break vectorization (loops with conditional `break` statements), and an improved `-O2` cost model. LLVM’s RISC-V backend has received intensive investment since then, in areas including VL tail folding and split register allocation between the RVV and scalar register files. LLVM 21 advances by extending the RISC-V backend to support a rich set of CPU models, including the SpacemiT scheduling model.

3 Methodology

We develop a set of hand-written RVV 1.0 assembly microbenchmarks ⁴ for assessing key RVV 1.0 instructions and for verifying *perf* performance profiling

⁴ <https://github.com/KTH-ScaLab/rvv-evaluation>

counters. Leverage those validated *perf* counters, we compare and analyze the performance difference of GCC 15 and Clang 21 in autovectorizing six representative proxy applications from HPC and ML domains on two RVV 1.0 testbeds.

Assembly Microbenchmarks. Since compiler-generated code may conflate micro-architectural behaviors with compiler decisions, we use a set of assembly microbenchmarks that issue precisely controlled sequences of RVV 1.0 instructions with explicit control of operand types and register configurations. We leverage the assembly codes to establish the performance ceiling in terms of raw throughput on the target testbed. Each assembly benchmark consists of a hand-written inner loop repeating a target RVV instruction for 10^8 times. The operands are pre-staged in vector registers to eliminate cold-start effects. Dependency among successive instructions is broken to expose peak issue throughput. If $VL < VLEN$ or mask operations are used, *vta* and *vma*, configured by *vsetvli*, will control the behavior of destination tail elements and inactive masked-off elements, respectively. We opt for the agnostic policy when preserving the tail/masked-off elements in the destination vector register is not required.

The first set of benchmarks targets memory instructions to support common access patterns. Unit-stride loads and stores (*vleN.v / vseN.v vd, (rs1)*) are used for sequential access patterns. Non-uniform access patterns are realized through two options: (1) strided loads and store (*vlseN.v / vsseN.v vd, (rs1)*), and (2) through masked vector loads (*vleN.v / vseN.v vd, (rs1), v0.t*) with an alternating mask pattern 1010... stored in *v0.t*. Indexed gather and scatter operations (*vluxei/ vsuxei*) are not evaluated because they have the same access behavior as *vlse/vsse* in the fixed-stride case, but introduce the additional index register and are seldom selected by the compiler auto-vectorization. The second set of benchmarks targets floating-point and integer arithmetic instructions. Assembly codes target vector addition (*vfadd.vv*), multiplication (*vfmul.vv*), fused multiply-add (*vfmac.vv*), and division (*vfdiv.vv*) in FP16 (*e16*), FP32 (*e32*), and FP64 (*e64*), and their integer counterpart instructions at 8-bit, 16-bit, 32-bit, and 64-bit element widths.

Performance Counter Calibration with Assembly Benchmarks. Unlike mature architectures such as x86 or AArch64, where performance counters are thoroughly documented, the hardware performance counters on RVV hardware through the Linux *perf* subsystem are implementation-defined [3]. Therefore, before using counter-derived metrics for analyzing RVV vectorization efficiency, we calibrate which events are reliable on this specific microarchitecture. In particular, we collect seven *perf* events: total retired instruction, vector instruction, vector ld/st instruction, FP ld/st instruction, and FP instruction. Table 1 summarizes the measurement of these events in 10 assembly benchmarks, where the target instruction sequences are known from assembly codes and their counts are presented in *Ref ins*. Take the *vfadd.vv* benchmark for example, a loop issuing N *vfadd.vv* must retire N vector FP instructions and a small number of extra scalar loop-control instructions. Thus, the total retired instructions as reported in *Retired ins*. should be close to but slightly higher than *Ref ins*.

Table 1: Perf event statistics for different assembly instructions.

Assembly bench.	Ref #ins.	Retired ins.	Vec. ld ins.	Vec. st ins.	Vec. ins.	FP ld ins.	FP st ins.	FP ins.
flw	1.28×10^{10}	1.31×10^{10}	16	16	55	1.28×10^{10}	696	1.28×10^{10}
lw	1.28×10^{10}	1.31×10^{10}	16	16	53	736	855	1613
vle.vv	1.28×10^{10}	1.31×10^{10}	1.28×10^{10}	17	1.28×10^{10}	662	738	2443
fsw	1.28×10^{10}	1.31×10^{10}	16	16	55	601	1.28×10^{10}	1.28×10^{10}
sw	1.28×10^{10}	1.31×10^{10}	16	16	53	736	855	1613
vse.vv	1.28×10^{10}	1.32×10^{10}	1108	1.28×10^{10}	1.28×10^{10}	662	738	2443
vfadd.vv	1.28×10^{10}	1.30×10^{10}	124	17	1.28×10^{10}	652	726	2.56×10^{10}
vmacc.vv	1.28×10^{10}	1.30×10^{10}	144	17	1.28×10^{10}	632	723	2.56×10^{10}
fadd	1.28×10^{10}	1.30×10^{10}	16	16	6.40×10^9	770	856	1.28×10^{10}
fmadd	1.28×10^{10}	1.30×10^{10}	16	16	6.40×10^9	770	856	1.28×10^{10}

A counter is deemed reliable if its reported value approximates the reference within a tolerance of 5% across five independent runs. This threshold is chosen to accommodate minor perturbations from interrupt handling and context-switch overhead, a known limitation in RVV performance monitoring [3]. The retired instruction achieves 98.4-99% accuracy on all 10 benchmarks. Similarly, vector ld/st and FP ld/st instructions only show $< 10^{-5}\%$ error. Counters whose reported values are beyond the tolerance are unreliable and thus excluded in the profiling analysis in Sections 5. Vector instruction, which records all vector instructions, is expected to be close to 0 in `fadd` and `fmadd` benchmark, shows an error of approximately 50%. A similar issue appears in FP instructions `vfadd.vv` and `vmacc.vv`, where the expected value is also near zero, but the real value shows an error of 100%.

Application Benchmarks. To evaluate auto-vectorization performance under realistic workload conditions, we select six proxy applications representative of dominant computational and memory patterns in scientific and ML workloads. Stream measures sustained memory bandwidth through simple element-wise kernels. SpMV exhibits irregular memory access via sparse matrix-vector multiplication, where indirect indexing and poor spatial locality make it latency-bound. DGEMM and SGEMM implement double- and single-precision dense matrix multiplication, respectively, whose loop structure is regular and compute-bound, representing ideal cases for autovectorization. YOLOv3 and AlexNet represent CNN inference workloads that mix regular convolution with non-linear activations and pooling. Together, these applications cover diverse patterns and exercise the various data precision characterized in the assembly microbenchmarks. Further, we evaluate a production-level application for simulating quantum computers developed by Google, called QSIM, to investigate the RVV compiler support for both auto-vectorization and RVV intrinsics. For this, we also provide a manually ported QSIM using RVV intrinsics for comparison⁵.

Compiler and Testbed Setup. GCC15.1.0 and Clang21.1.1 are used. All compiler configurations are augmented with `"-O3/-Ofast -fopenmp"`. The first version of compilation, *non-vec*, uses flag `"-march=rv64gc -fno-tree-vectorize"` in GCC15 and `"-mllvm -scalable-vectorization=off"` in Clang21, to disable the vectorization. The second version, *auto-vec*, uses flag `"-march=rv64gcv_zfh_zvfh"` in GCC15 and `"-march=rv64gcv_zfh_zvfh -mllvm -scalable-vectorization=on"`

⁵ https://github.com/KTH-ScaLab/qsim_rvv

in Clang21. This version enables the autovectorization and uses the default LMUL setting in each compiler. In a variant, we also specify LMUL, using "-mrvv-max-lmul" in GCC15 and "-mllvm -riscv-v-register-bit-width-lmul" in Clang21.

The testbeds consist of Milk-V Jupiter and BananaPi BPI-F3, both are based on the Spacemit(R) X60 CPU with 8 cores implementing 2×256 -bit RVV1.0 support, running at 1.6 GHz (BananaPi) and 1.8 GHz (Jupiter) frequency. The memory hierarchy includes 32 KB L1 instruction and 32 KB L1 data caches per core, and a shared 2×512 KB L2 caches. The systems are equipped with 16 GB of LPDDR4X (Milk-V Jupiter) and LPDDR4 (BPI-F3) main memory. We use the perf in Linux kernel 6.1.15 and kernel 6.6.63 on the BSC testbed.

4 Understanding Basic RVV Instructions

We start our evaluation with two categories of vector instructions, i.e., data access instructions and arithmetic instructions. For ld/st instructions, we investigate three access patterns, covering sequential, non-unit, and tailing elements. While the sequential ld/st can be achieved with the `vle/vse` instructions, non-unit and tailing elements can be achieved in different ways, as illustrated in Figure 1. Thus, we design the assembly benchmark for each variant to identify the recommended choice for programmers.

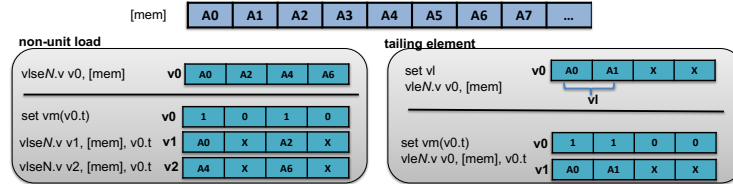


Fig. 1: The diagram of non-unit and tailing vector load

For a sequential load pattern, unit-stride load `vle8` achieves the highest throughput of 28.4 Gops/s on Jupiter (25.2 Gops/s on BPI-F3), and its 16|32|64-bit variants scale the throughput proportionally to 14.2, 7.1, 3.55 Gops/s, respectively. This throughput approaches the hardware's theoretical peak closely.

For non-unit load patterns, we focus on the stride access patterns. For instance, for stride=2, `mem[0]`, `mem[2]`, `mem[4]`, ..., `mem[2*i]` should be accessed, shown in Figure 1. We design three benchmarks to compare different instructions to achieve the same access pattern. In the first benchmark, vector stride load instruction `vlse` is used to gather elements from memory with a stride of 2 into a vector register. The second benchmark uses unit load `vle` to access contiguous elements from `mem` and a mask register (1010) to only enables the corresponding positions of required elements 0, 2, 4, ... in the destination vector register. To load the same number of elements as a single `vlse`, this method requires two masked `vle` instructions. Moreover, the configuration instructions to generate masks are added at initialization stage. All additional overheads are included in the throughput measurements. Finally, the third benchmark adds a

reference to a scalar implementation, where scalar loads are used to read elements with a constant stride from memory to scalar registers.

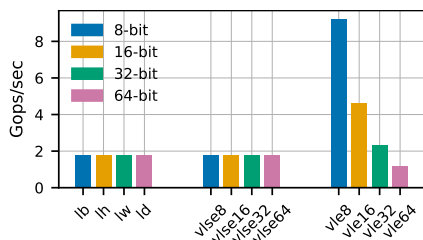


Fig. 2: The peak throughput of non-uniform load instructions on Jupiter.

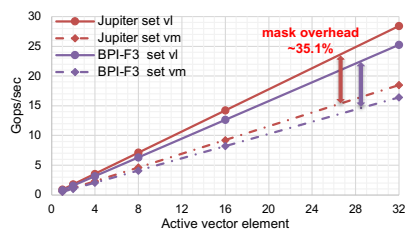


Fig. 3: Compare the performance of tailing elements via setvl and mask operations on BPI-F3 and Jupiter.

Figure 2 presents the results of the three benchmarks for stride loads on Jupiter. The results show `vlse` and scalar are consistent at 1.78 Gops/s in any variants. `vle` with mask achieves the best performance of 9.2 Gops/s at 8-bit precision and the throughput scales up with reduced data precision. In 64-bit data precision, the throughput of the `vle` with mask is $0.65\times$ lower than `vlse`. Store has identical performance as load at all instructions, except `vsse32` only achieving 1.2 Gops/s, thus omitted from Figure 2.

RVV provides a unique way of handling tail elements by setting its active vector length VL, in addition to the masked predicate operations. To guide the selection between these two options, we design two assembly benchmarks to compare these two ways of handling irregular vector lengths. Shown in Figure 1(b), we load `v1` elements with useless tail element in destination vector register, where `v1 < VLMAX`. The first benchmark uses the `vset{i}v1{i}` instruction to change the VL. The second benchmark achieves the same goal by setting the mask register `v0.t`. Figure 3 presents the performance comparison of these two methods. Setting `v1` reaches about 28.4 Gops/s and 25.2 Gops/s at 32 active elements, whereas mask achieves only 18.5 Gops/s and 16.4 Gops/s on Jupiter and BPI-F3, respectively. A constant 35.1% performance loss in masked operations at any active vector elements. The mask configuration introduces negligible cost, as only three additional instructions are required in initialization. The observed overhead mainly comes from vector execution, representing the inefficiency in executing the masked vector instructions in vector units.

Evaluating peak arithmetic throughput is essential to establish the performance ceiling and determine whether the 2×256 -bit vector pipelines deliver the theoretical throughput across different element sizes. In this evaluation, we focus on floating-point (FP16|32|64) and integer (INT8|16|32|64) operations important for scientific and machine learning workloads. We design each microbenchmark consisting of a tight, dependency-free loop of a single RVV 1.0 instruction, e.g., (`v(f)add.vv`, `v(f)mul.vv`, `v(f)macc.vv`, `v(f)div.vv`), issued at different LMUL. The benchmark preloads operands into vector registers to eliminate memory latency and repeats 4×32 instructions with `v0-v32` as destination per

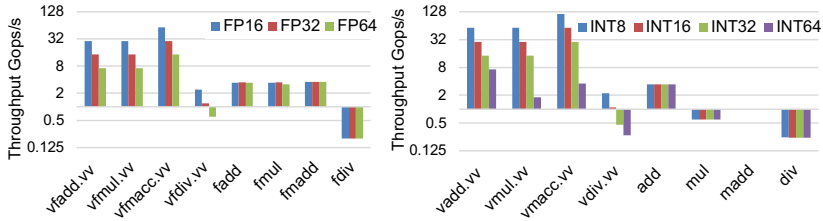


Fig. 4: The peak throughput of selected vector and scalar arithmetic instructions in FP16/32/64 and INT8/16/32/64 on Jupiter.

iteration and 10^8 iterations to reach steady operation throughput. We also measure the scalar counterparts ((f)add, (f)mul, (f)madd) identically to provide the baseline for quantifying the vector speedup. Figure 4 summarizes the measured throughput.

The result reveals that the fused multiply-add vector operation achieves the highest throughput of all measured instructions, with FP16 reaching 57.5 Gops/s, 28.7 Gops/s for FP32, and 14.4 Gops/s for FP64, consistent with the expected doubling of element count per vector register as precision is halved. The fused multiply-add `vfmacc.vv` at FP32 nearly matches the throughput of `vfmul.vv` and `vfmul.vv`, demonstrating that the hardware can issue fused operations at full vector throughput. This is favourable for BLAS-like kernels that are dominated by DAXPY and GEMM patterns. The scalar counterparts, `fadd`, `fmul`, and `fmadd` instructions achieve only 3.1-3.5 Gops/s regardless of precision, indicating $16\times$ throughput advantage of the vector variants for FP16. For INT arithmetic instructions, `vmul.vv` scales proportionally 51.1, 25.6, 12.8 Gops/s with INT8-32 and only 1.6 Gops/s for INT64, while scalar `mul` only achieves a constant at 0.53 Gops/s, even worse than `fmul`, indicating the inefficient scalar multiplier support in ALU. Both `vdiv.vv` and scalar `div` show very low throughput (0.22- 1.97 Gops/s), reflecting the high latency of the divider. This encourages the programmers and compiler optimization to replace division with shift or multiplication if possible.

5 GCC15 and Clang21 Support in Proxy Apps

While the assembly benchmark helps understand performance ceiling, evaluating proxy applications from scientific and ML workloads is necessary to assess whether autovectorization translates into application level speedups. We evaluate six proxy applications compiled with GCC 15 and Clang 21 into non-vectorized and autovectorized binaries. We report all speedups normalized against the non-vectorized GCC 15 baseline. We evaluate performance on both BPI-F3 and Jupiter and observe consistent conclusions across the two platforms. Therefore, unless otherwise stated, the following results presented are from Jupiter.

Figure 5a presents an overview of achieved speedup by GCC15 and Clang21 on Milk-V Jupiter. The autovectorization benefits are highly application-dependent.

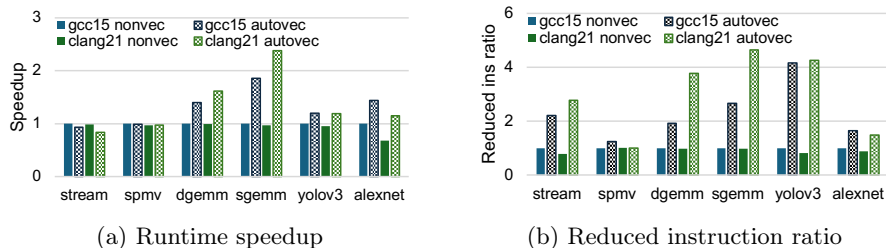


Fig. 5: The performance by GCC 15 and Clang 21 autovectorization across six proxy apps on Jupiter, normalized by the GCC 15 nonvec baseline

Clang 21 achieves more speedup than GCC 15 in `sgemm` and `dgemm`, where `sgemm` gains approximately $2.4\times$ speedup with Clang 21 and around $1.85\times$ with GCC 15. While both compilers can effectively vectorize `gemm`'s regular inner loop, Clang 21 yields better speedup probably because of its SpacemiT X60 specific instruction scheduling model and LMUL selection. In the YOLOv3 and AlexNet benchmarks, GCC 15 achieves better speedup than Clang 21. For instance, AlexNet shows approximately $1.45\times$ speedup with GCC 15 but only $1.2\times$ speedup with Clang 21. Stream and SpMV, two memory-bound benchmarks, show no autovectorization benefit from both compilers. While GCC 15 achieves the same performance as the non-vectorized version, Clang 21 even decreases the performance to be worse than the non-vectorized version in stream, i.e., the Clang 21 vectorized stream is about 20% slower than Clang 21 non-vectorized version. A notable observation from comparing the non-vectorized baseline is that Clang 21 is consistently slightly below 1.0, suggesting that GCC 15 generates better scalar codes. Figure 5b reveals that instruction reduction ratio is a strong predictor of speedup, but the relationship is application-dependent. SGEMM and YOLOv3 show the largest reductions in instructions, with Clang 21 autovec, retiring $4.7\times$ and $4.3\times$ fewer instructions, respectively than the GCC 15 scalar baseline. While the reduction in instructions in SGEMM and YOLOv3 confirms that wide vector operations successfully amortize computation across multiple elements, stream also exhibits a large instruction reduction ($2.2\times$ for GCC 15 and $2.8\times$ for Clang 21) but without a corresponding speedup, which is as expected for its memory-bandwidth nature. The DGEMM and AlexNet reductions are moderate, i.e., approximately $2.0\times$ and $1.6\times$ for GCC 15 autovec. They correlate with their moderate speedups.

SpMV shows nearly no instruction reduction under either compiler in RVV. For comparison, we evaluate the same kernel on another VLA architecture, ARM SVE, where a $1.99\times$ instruction reduction by GCC auto-vectorization is observed on a 128-bit SVE Neoverse V2 core. This discrepancy suggests that the automatic vectorization support for RVV remains less mature and requires further improvements in the compiler toolchains.

Comparing the two compilers, Clang 21 consistently reduces more instructions than GCC 15 across all vectorized applications, but this advantage is most effectively converted into speedup when the application is compute-bound. For



Fig. 6: The breakdown load/store instructions in BPI-F3

memory-bound workloads, the instruction savings go largely unrealized as the LPDDR4X channel memory subsystem becomes the bottleneck.

Profiling Analysis. In this section, we leverage those reliable performance counters to decompose the retired instruction mix into vector load and store, floating-point load and store events to compare the instruction breakdown in different compiler-vectorized versions. The profiling result present in Figure 6 reveals that autovectorization dramatically reduces the total number of memory access instructions across all six applications, with the most reductions occurring in DGEMM and SGEMM.

In SGEMM, the non-vectorized baseline is dominated by a large portion of FP ld/st instructions, which collapse to a small fraction under autovectorization, as each vector load can replace multiple scalar FP loads, indicating both GCC 15 and Clang 21 can effectively recognize such patterns. In Stream, the autovectorized version successfully eliminates most scalar load/store to a small residual of vector load and store instructions. However, although Clang 21 achieves a larger instruction reduction for STREAM, the observed performance is worse, likely caused by unsuitable memory access order after vectorization. As an in-order CPU model, the performance of Spacemit(R) X60 is sensitive to the static instruction scheduling by compilers. SPMV is the notable exception: both non-vectorized and autovectorized versions retain a similar instruction mix with a dominant FP load component and negligible vector memory instructions in Clang 21. Although vector load dominates in GCC 15 and obviously reduces the FP ld/st instructions, the total instructions are almost not reduced according to Figure 5b. Further analyzing the compiler vectorized report, for the indexing memory access `vector[colIndex[col]]`, Clang 21 can not identify array bounds in SPMV, avoiding any parallelization optimization techniques. GCC 15 can vectorize part of the code using variable-length unit vector load, but additional missed optimizations associated with statement clobbers memory, avoiding further vectorization in fused-multiply-add.

Comparing GCC 15 and Clang 21, Clang 21 without vectorization generates more scalar memory instructions, likely due to differences in scalar loop unrolling and scheduling policies. Under autovectorization, however, Clang 21 reduces its instruction stack more aggressively than GCC 15 in DGEMM, SGEMM, and the ML workloads. The autovectorized Clang 21 bar for SGEMM approaches the smallest total instruction count of any configuration, consistent with its larger

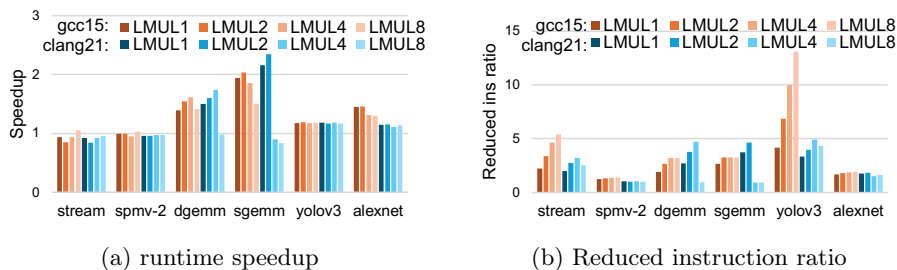


Fig. 7: The impact of LMULs selection on Jupiter, normalized by GCC 15 nonvec

instruction-reduction ratio and higher speedup. For YOLOv3 and AlexNet, GCC 15 autovec and Clang 21 autovec produce nearly identical instruction mixes, which explains why their speedups converge for these workloads despite the larger scalar-code difference between the two compilers.

Impact of LMUL in GCC15 and Clang21. Although autovectorization defaults to a compiler-chosen LMUL value, the choice of LMUL is known to affect performance profoundly by trading register count against element throughput per instruction [10, 6]. Higher LMUL values process more elements per cycle but reduce the number of available architectural vector registers from 32 (at LMUL=1) down to just 4 (at LMUL=8), trading off between instruction-level parallelism and register pressure. Therefore, we sweep LMUL in these proxy applications to determine whether the compiler’s default LMUL selection is optimal for each workload and to guide users toward performance-portable choices when targeting the SpacemiT microarchitecture.

Figure 7 shows that the optimal LMUL setting is application- and compiler-dependent for performance. For SGEMM, Clang 21 at LMUL=2 achieves the highest speedup, approximately $2.35\times$. However, the performance degrades sharply at LMUL=8, to around $0.85\times$, below scalar performance, due to the high risk of register spilling. GCC 15 on SGEMM and DGEMM benefits from increasing LMUL up to $LMUL = 4$, reaching approximately $2.0\times$ and $1.6\times$ respectively. One hypothesis is that the conservative unrolled and vectorized loop strategy in GCC 15 allows it to better tolerate the higher register pressure caused by larger LMUL. Stream and SPMV remain near or below $1.0\times$ across all LMUL values for both compilers. This is expected because their bottlenecks at memory bandwidth and irregular memory access latency, respectively, could be even exacerbated by widening vector register groups. For most applications, selecting LMUL=1 or LMUL=2 provides better performance. Larger LMUL values increase register pressure and may trigger register spilling, which significantly degrades performance. This observation suggests that the compiler’s default LMUL selection strategy is close to the optimal, and tuning the larger LMUL in GCC 15 can get more performance gains than Clang 21.

Instruction reduction does not always translate into performance speedup, for example, YOLOv3 by GCC shows a proportional instruction reduction ratio with LMUL ($13.1\times$ at LMUL=8), closer to the theoretical value. However, the speedup of YOLOv3 and AlexNet is insensitive to LMUL for both compilers,

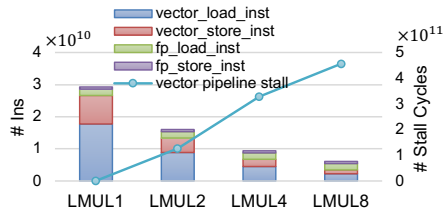


Fig. 8: Yolov3 profiling analysis on the impact of LMULs

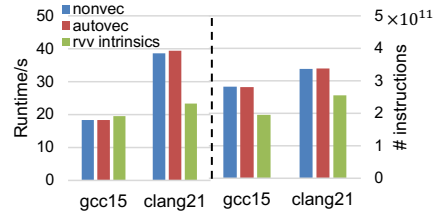


Fig. 9: The comparison of Qsim across 3 versions using 8 cores

remaining 1.2 \times , implying that their performance is constrained by some other factors other than VL. To understand the execution bottleneck of YOLOv3 in larger LMUL, we further break down its profiling results. We profile the instruction composition to verify the effectiveness of vectorization, shown in Figure 8. The profiling results show that scalar load/store instructions are largely replaced by vector load/store instructions, indicating that the kernel has been effectively vectorized. However, despite the reduction in total instruction and ld/st instructions, no speedup benefit is observed. To investigate the bottleneck, we profile the vector pipeline behavior. Figure 8 reflects that the vector store pipeline cycles increase linearly with larger LMUL, rising from 2.3×10^8 at LMUL1 to 4.6×10^{11} at LMUL8. This indicates that aggressive vector register grouping increases pressure on the vector pipeline, eventually exceeding its peak throughput. Consequently, instructions must wait for available vector pipeline resources to execute and commit, resulting in pipeline stalls.

6 Qsim Quantum Circuit Simulator

Google’s Qsim [14] is a Schrodinger full state-vector simulator, which is highly optimized for FP32 arithmetic. Previous porting on ARM SVE backends achieves high performance [17]. Qsim uses interleaving layout to store the real and imaginary parts of the complex value for each state vector. The interleaved memory access pattern in Qsim makes compiler auto-vectorization difficult. To enable effective vectorization on RISC-V platforms, we port the implementation using RVV intrinsics via VLEN-adaptive memory layout adjustment and fine-grained vectorized loop by setting proper masks in operation to disable useless elements per vector instructions.

The autovec version shows nearly identical runtime to the nonvec version in GCC 15(18.3 s) and Clang 21(39.4 s) in Figure 9 and no instruction reduction is observed, indicating that the compiler fails to effectively vectorize Qsim. The RVV intrinsics implementation significantly reduces the instruction count on both compilers, achieving around $1.4 \times$ reduction ratio with GCC 15 and $1.3 \times$ with Clang 21. However, the runtime with GCC 15 is even slightly longer than nonvec version, whereas Clang 21 achieves $1.6 \times$ speedup compared to its own nonvec version. Despite the improvement from RVV intrinsics in Clang 21, its absolute runtime remains about $1.2 \times$ slower than GCC 15, and the generated

instructions is $1.2-1.3 \times$ higher. Qsim results highlight the limitations of current compiler auto-vectorization for applications with complex memory access patterns as Qsim. GCC 15 performs better than Clang 21 in this real-world workload. Manual RVV intrinsics can effectively reduce instruction counts, but the achieved performance is strongly dependent on compiler code generation quality, requiring further optimization and compiler support for VLA architectures.

7 Related Work

Understanding and profiling the performance of RVV processors is critical for both architectural design and software optimization. Previous studies evaluated and analyzed the performance of a set of RISC-V processors equipped with RVV, ranging from high-performance computing [5, 10] to machine learning [8, 7] workloads. For the feasibility and maturity of compiler support for auto-vectorization, several works evaluated the performance comparison between the GNU and LLVM compiler toolchains for RISC-V RVV across TSVC scientific loops and real applications [6, 9]. Adit et al. [1] emphasized a significant performance gap between auto-vectorized and hand-optimized code for the RVV extension by examining LLVM’s support for both RVV and VLS-style Intel AVX and ARM Neon. Peccia et al. [12] auto-tuned the vector instructions for AI workloads by integrating the scheduler into the TVM compiler.

Several studies explored the performance on specific RVV hardware via rewriting assembly and intrinsics [4, 11]. Since high-end RVV hardware is still emerging, evaluating on the cycle-accurate simulators such as GEM5 [8, 15] is used to profile the detailed vector activities and explore the RVV design space. Ref [3, 18] compare three instrumentation methods: inline assembly CSR reads, Linux *perf*, and PAPI and proposed a Linux 6.10 kernel patch to toggle between per-managed and direct CSR-based counter access.

8 Conclusion

In this work, we first developed assembly benchmarks to calibrate vector-related *perf* events on BananaPi RVV hardware. Evaluating the latest GCC 15 and Clang 21 support for RVV 1.0 auto-vectorization and intrinsics across six scientific and ML applications, we find that GCC 15 produces more stable and efficient code generation than Clang 21. Default LMUL selection proves near-optimal in most cases, though GCC 15 shows greater potential for performance gains through larger LMUL tuning than Clang 21. We further developed an RVV backend for Google’s Qsim quantum circuit simulator using RVV intrinsics, where GCC 15 again outperforms LLVM 21 on this complex, real-world workload. Nevertheless, compared to mature compiler support for ARM SVE, both compilers require continued development to fully realize the performance potential of RVV 1.0.

Acknowledgments. This work was performed under the auspices of the U.S. Department of Energy by Lawrence Livermore National Laboratory under Contract DE-AC52-07NA27344 under LDRD Project 24-ERD-047. This research is supported by the European Commission under the Horizon project HIGHER (101189612). This research is supported by the RISC-V ExCALIBUR project at EPCC. The authors have no competing interests to declare that are relevant to the content of this article.

References

1. Adit, N., Sampson, A.: Performance left on the table: An evaluation of compiler autovectorization for risc-v. *IEEE Micro* **42**(5), 41–48 (2022)
2. Asanovic., K.: <https://github.com/riscv/riscv-v-spec/releases/tag/v1.0> (2021)
3. Banchelli, F., et al.: Risc-v in hpc: a look into tools for performance monitoring. In: *International Conference on High Performance Computing*. pp. 562–575 (2025)
4. Bernstein, O.: RISC-V Vector benchmark. <https://github.com/camel-cdr/rvv-bench>
5. Brown, N., et al.: Is RISC-V ready for hpc prime-time: Evaluating the 64-core sophon SG2042 RISC-V CPU. In: *Proc. SC’23 Workshops*. pp. 1566–1574 (2023)
6. Carpentieri, et al.: A performance analysis of autovectorization on rvv risc-v boards. In: *Proc. PDP*. pp. 129–136 (2025)
7. Garcia, A.M., et al.: Inference performance of large language models on a 64-core risc-v cpu with silicon-enabled vectors. *Future Generation Computer Systems* p. 108242 (2025)
8. Gupta, S.R., et al.: Accelerating CNN inference on long vector architectures via co-design. In: *2023 IEEE International Parallel and Distributed Processing Symposium*. pp. 145–155. IEEE (2023)
9. Lai, H.M., et al.: RISC-V vectorization coverage for HPC: A TSVC-based analysis. In: *Proceedings of the SC’25 Workshops*. pp. 1676–1683 (2025)
10. Lee, J.K., et al.: Test-driving risc-v vector hardware for hpc. In: *International Conference on High Performance Computing*. pp. 419–432. Springer (2023)
11. Lin, J.K., et al.: Rewriting and optimizing vector length agnostic intrinsics from arm sve to rvv. In: *Proc. 53rd ICPP Workshops*. pp. 38–47 (2024)
12. Peccia, F.N., Haxel, F., Bringmann, O.: Tensor program optimization for the RISC-V vector extension using probabilistic programs. In: *2025 IEEE/ACM International Conference On Computer Aided Design (ICCAD)*. pp. 1–9. IEEE (2025)
13. Perotti, M., et al.: A “new ara” for vector computing: An open source highly efficient risc-v v 1.0 vector processor design. In: *ASAP*. IEEE (2022)
14. Quantum AI team: qsim (Jun 2025), <https://doi.org/10.5281/zenodo.4067237>
15. Ramírez, C., et al.: A risc-v simulator and benchmark suite for designing and evaluating vector architectures. *TACO* **17**(4), 1–30 (2020)
16. Shi, R., et al.: ARM SVE unleashed: Performance and insights across hpc applications on nvidia grace. In: *European Conference on Parallel Processing*. pp. 33–47. Springer (2025)
17. Shi, R., et al.: High-performance vector-length agnostic quantum circuit simulations on arm processors. In: *International Parallel and Distributed Processing Symposium*. IEEE (2026)
18. Vizcaino, P., et al.: Designing a qemu plugin to profile multicore long vector risc-v architectures: Rave. *Future Generation Computer Systems* p. 108100 (2025)